Experimental Eye Research 132 (2015) 91–100

Contents lists available at ScienceDirect

Experimental Eye Research

journal homepage: www.elsevier.com/locate/yexer

Acellular human corneal matrix sheets seeded with human adipose-derived mesenchymal stem cells integrate functionally in an experimental animal model

Jorge L. Alio del Barrio [a], Massimo Chiesa [b], Nerea Garagorri [c], Nerea Garcia-Urquia [c], Jorge Fernandez-Delgado [d], Laurent Bataille [e], Alejandra Rodriguez [e], Francisco Arnalich-Montiel [a], Tomasz Zarnowski [f], Juan P. Álvarez de Toledo [g], Jorge L. Alio [e], Maria P. De Miguel [b, *]

[a] Ophthalmology Department, Ramon y Cajal Hospital, Madrid, Spain
[b] Cell Engineering Laboratory, IdiPAZ, La Paz Hospital Research Institute, Madrid, Spain
[c] Tecnalia Research & Innovation, Health Division-Biomaterials Area, Mikeletegi Pasealekua 2, 20009 Donostia-San Sebastian, Spain
[d] Department of Plastic and Reconstructive Surgery, Santa Cristina Hospital and Centrocim, Madrid, Spain
[e] Vissum Ophthalmological Institute and Miguel Hernandez University, Alicante, Spain
[f] Lublin Eye Bank, Lublin, Poland
[g] Eye Bank of Barraquer Ophthalmology Center, Barcelona, Spain

ARTICLE INFO

Article history:
Received 20 February 2014
Received in revised form
4 June 2014
Accepted in revised form 23 January 2015
Available online 24 January 2015

Keywords:
Adipose derived stem cells
Cornea
Decellularization
Recellularization
Lamellar corneal transplant
Corneal stroma regeneration
Tissue engineering

ABSTRACT

Purpose: To evaluate the in vivo biocompatibility of grafts composed of sheets of decellularized human corneal stroma with or without the recellularization of human adipose derived adult stem cells (h-ADASC) into the rabbit cornea.

Methods: Sheets of human corneal stroma of 90 μm thickness were decellularized, and their lack of cytotoxicity was assayed. The recellularization was achieved by the injection of 2×10^5 labeled h-ADASC in the graft followed by five days of cell culture. The grafts were implanted in vivo into a stromal pocket at 50% depth. After a triple-masked three-month follow-up, the animals were euthanized and the bio-integration of the graft, the viability of the stem cells and the expression of keratocan (human keratocyte-specific protein) were assessed.

Results: The decellularized stromal sheets showed an intact extracellular matrix with a decellularization rate of 92.8% and an excellent recellularization capacity in vitro with h-ADASC. A complete and stable graft transparency was observed during the full follow-up, with absence of any clinical sign of rejection. The postmortem analysis demonstrated the survival of the transplanted human stem cells inside the graft and their differentiation into functional keratocytes, as assessed by the expression of human keratocan.

Conclusions: We report a new model of lamellar keratoplasty that requires only a simple and safe procedure of liposuction and a donor allogeneic cornea to provide an optically transparent autologous stromal graft with excellent biocompatibility and integration into the host tissue in a rabbit model.

1. Introduction

Most corneal diseases primarily or secondarily involve the corneal stroma, a layer that accounts for 90% of the corneal thickness. In the last decade, full thickness or penetrating keratoplasty has been partially displaced by techniques that selectively replace diseased layers, such as deep anterior lamellar keratoplasty (DALK) for the stroma (Shimmura and Tsubota, 2006). DALK techniques avoid endothelial rejection, which is the most common cause of

Abbreviations: h-ADASC, human adipose derived adult stem cells; ECM, extracellular matrix; RT, room temperature; OD, optical density.

* Corresponding author. Cell Engineering Laboratory, IdiPaz, La Paz Hospital Research Institute, Paseo Castellana 261, Madrid 28046, Spain.
E-mail address: mariapdemiguel@gmail.com (M.P. De Miguel).

http://dx.doi.org/10.1016/j.exer.2015.01.020
0014-4835/

graft failure, but they still have the disadvantages of primary immune stromal rejection, a shortage of corneas and high postoperative astigmatism due to the suture (Watson et al., 2006; Krumeich et al., 2008). Our purpose is to avoid all these drawbacks by developing a new approach to autologous lamellar keratoplasty, beginning with an allogeneic graft.

The cellular compartment of the corneal stroma is composed primarily of keratocytes, which are mitotically quiescent cells with a flat and dendritic morphology that secrete collagens and keratan sulfate proteoglycans, such as keratocan (Michelacci, 2003). Keratocan is known as a keratocyte-specific marker because it is exclusively expressed by adult keratocytes (Carlson et al., 2005). Cell-based therapy of the cornea is a promising therapeutic approach, but using autologous human keratocytes has major drawbacks, such as damage to the donor cornea, lack of cells and inefficient cell subculture (De Miguel et al., 2010). In the last few years, some research has been done searching for an extraocular source of cells for this purpose (Arnalich-Montiel et al., 2008; Espandar et al., 2012). Human adult adipose tissue has been demonstrated to be an ideal source of autologous stem cells, as it satisfies all the requirements: easy accessibility to the tissue, high cell retrieval efficiency and the ability of its stem cells, known as "human adipose derived adult stem cells" (h-ADASC), to differentiate into multiple cell types (keratinocytes, osteoblasts, chondroblasts, myoblasts, hepatocytes, neurons, etc.) (De Miguel et al., 2010; Arnalich-Montiel et al., 2008). This cellular differentiation occurs under the effect of specific stimulating factors or environments for each cell type, avoiding the mix of multiple types of cells in different niches. In addition, these cells have shown immunomodulatory properties in syngeneic, allogeneic and even xenogeneic scenarios (De Miguel et al., 2012; Fang et al., 2007; Puissant et al., 2005). In a previous study from our group (Arnalich-Montiel et al., 2008), we found that human ADASC transplanted into damaged rabbit corneas were capable of functionally differentiating into corneal keratocytes. They produced collagens and keratocan proper of the corneal stroma, however, insufficient collagen production was achieved to restore the corneal thickness and transparency.

Tissue engineering of functional corneal equivalents has been developed, however, the complex structure of the corneal stroma has not yet been replicated, and there are well-known drawbacks to the use of synthetic scaffold-based designs: strong inflammatory responses are induced upon their biodegradation, and nearly all polymer materials cause a nonspecific inflammatory response (Ruberti and Zieske, 2008; Griffith et al., 2002). The extracellular matrix (ECM) is by definition nature's ideal biologic scaffold material because it is custom designed and manufactured by the resident cells of each tissue and organ. Components of the ECM are generally conserved among species and are tolerated well even by xenogeneic recipients. Recently, several corneal decellularization techniques have been described, which provide an acellular corneal ECM (Daniel et al., 2005; McFetridge et al., 2004; Shao et al., 2012, 2010). However, to the best of our knowledge, there are no published studies that have tested human decellularized stromal grafts with posterior recellularization with human stem cells in vivo.

The aim of this study was to evaluate the in vivo biocompatibility of grafts composed of sheets of decellularized human corneal stroma with or without subsequent human ADASC recellularization inside the rabbit cornea.

2. Materials and methods

2.1. Isolation and culture of h-ADASC

Lipoaspirate from two female donor patients undergoing elective liposuction was obtained by a plastic surgeon. The isolation protocols and usage of the tissue were approved by the institutional Review Board of the hospital, and stored in the Biobank of La Paz Hospital. Oral and written informed consent was obtained from the patients. Active infection by HIV, hepatitis C virus and syphilis was ruled out by serological analyses. The lipoaspirate obtained was washed extensively with phosphate-buffered saline, digested, and processed as reported previously (Zuk et al., 2001). The pellet obtained was cultured in a noninductive medium consisting of Dulbecco's modified Eagle's medium (DMEM; Gibco-BRL, Grand Island, NY, USA) containing 1 mM sodium pyruvate and 2 mM glutamine (Sigma–Aldrich, St. Louis, MO, USA), 10% fetal bovine serum (FBS; Whittaker, Walkersville, MD, USA), and 100 U/ml penicillin G and streptomycin solution (Gibco-BRL). This protocol has been demonstrated to be effective in isolating h-ADASC capable of multipotent lineage differentiation by a previous study of our group (Arnalich-Montiel et al., 2008).

2.2. Human corneal stroma decellularization

2.2.1. Tissue procurement

Twenty-two adult human corneas that were rejected for human transplantation due to positive viral serology or non-viable epithelium or endothelium were used: 25% showed positive viral serology (2 corneas were HIV positive and 3 corneas were hepatitis B positive) and 75% showed non-viable epithelium or endothelium (10 corneas with non-viable epithelium and 7 corneas without viable endothelium). Among the 22 corneas, 73% came from the International eye bank of Lublin (Lublin, Poland) and the remaining corneas (27%) came from the eye bank of Centro de Oftalmología Barraquer (Barcelona, Spain). All donors were of white race, with an average age of 45.1 years (SD 12.1), 67% men and 33% women. Directive 2004/23/EC on setting standards of quality and safety for the donation, procurement, testing, processing, preservation, storage and distribution of human tissues and cells; and Directive 2006/17/EC of the Council as regards certain technical requirements for the donation, procurement and testing of human tissues and cells were followed.

2.2.2. Preparation of corneal sheets and decellularization protocol

The corneas were extracted and transported in CorneaMax® medium (Eurobio) from the eye banks, where they were included in cryomolds (Cryomold, Tissue-Tek, Sakura, Japan) with OCT (Tissue-Tek) and stored at −20 °C. The corneas were cut with a cryotome (CM1950, Leica, Spain) in sheets of 90 μm thickness, and washed in PBS (Sigma) supplemented with 1% antibiotic-antimicotic (15400062, Gibco).

The decellularization protocol was based on the method developed by members of our group (Ponce Márquez et al., 2009). The samples were immersed in 1% (wt/vol) sodium dodecyl sulfate solution (SDS; Sigma) with a protease inhibitor cocktail (P8340, Sigma), and incubated in vacuum conditions on an orbital shaker (75 rpm) for 12 h at room temperature (RT). Later, the sheets were washed 8 times in PBS with 1% antibiotic-antimicotic in the same conditions for 1 h at RT. To remove DNA, the sheets were incubated in DNAase (Benzonase® Nuclease 6.5 U/mL, Merck) in PBS with protease inhibitor cocktail in the same conditions at 37 °C for 72 h. Finally, the sheets were washed 15 times in PBS with 1% antibiotic-antimicotic in the same conditions for 48 h at RT. The final sheets were conserved in CorneaMax® (Eurobio).

2.2.3. Verification of cell removal

The cell removal was verified by determining the DNA content through DAPI staining of serial sections of the sheet (Molecular Probes/Invitrogen, Eugene, OR, USA) and quantification by the Picogreen Assay kit (Molecular Probes/Invitrogen). In brief, the

control and the decellularized corneal sheets were digested with proteinase K (Qiagen) at 50 °C for 3 h, and the DNA was extracted with a DNA Mini kit (Qiagen). The DNA quantification was performed according to the manufacturer's instructions.

2.2.4. Evaluation of cytotoxicity of the sheets

A test for in vitro cytotoxicity was performed to determine whether the extracts from the decellularized corneal sheets could cause cytotoxicity due to chemical remnants from the decellularization protocol. The corneal sheet, cytotoxic material (Polyvinyl chloride with tin), non-cytotoxic material (Polyethylene) and medium (control medium) were incubated with MEM containing 10% FBS (Sigma) at 37° for 24 h, then cultured with a lung fibroblast cell line (ATCC CCL-171), seeded in 96-well plates (10^4 cells/well). The standard lung fibroblast cell line that is used to assess the in vitro toxicity of medical devices under the international norm UNE-EN-ISO-10993-5-2009 was used. The cellular cytotoxicity was quantitatively determined at 24 h by WST-1 (Cell Proliferation Reagent, Roche). The optical density (OD) at 450 nm was measured in a microplate reader (PowerWake XS, Biotek). The OD values were converted into values of viability using the average value of the control medium as reference. The statistical significance was assessed by Student's t-test at $p < 0.05$.

2.3. Recellularization of human corneal decellularized stromal sheets

The h-ADASC were incubated with a 1:200 dilution of dialkylcarbocyanine fluorescent solution chloromethyl-benzamide (Vybrant CM-DiI, Molecular Probes) in D-PBS for 10 min and then washed 3 times in PBS, to fluorescently label all intracellular membranes (the organelles) except the plasma and nuclear membranes. The cells were trypsinized and resuspended in Hanks' balanced salt solution (HBSS; Gibco), seeded by injection (2×10^5 cells in 500 μl) in 10 different points over both surfaces of each sheet and either used for transplantation 24 h later or cultured for 5 weeks, changing the culture medium every 48 h.

2.4. Implantation of recellularized human corneal sheets in rabbit corneas

The animal studies were performed in accordance with the guidelines set forth by the animal research committees at Vissum Ophthalmological Institute of Alicante (Spain), La Paz Hospital (Spain), and in accordance with the standards of the Association for Research in Vision and Ophthalmology (ARVO) for animal experimentation (ARVO Statement for the Use of Animals in Ophthalmic and Vision Research). To evaluate the biointregation and biosafety of recellularized human corneal stromal sheets transplanted into the rabbit cornea, a controlled and triple-masked experiment was performed using 18 adult New Zealand White rabbits (Granja San Bernardo, Navarra, Spain).

2.4.1. Surgical procedure and postsurgical treatment

The animals were anesthetized with a combination of intramuscular ketamine (35 mg/kg) and Xilacine (10 mg/kg). The rabbits were placed under an operating microscope, and after a superior corneal paralimbar preincision of 5 mm length and 200 μm depth made with a 45° blade, a corneal half-depth intrastromal pocket of 7 mm in diameter was created by a minicrescent blade (Sharptome™, Sharpoint) at the central cornea to allow space for the human stromal sheet, which was placed unfolded and centered inside the rabbit cornea. The incision was then closed with two interrupted 10/0 nylon sutures. Topical ciprofloxacin 0.3%, cyclopentolate hydrochloride 0.5% and subcutaneous buprenorphine were applied at the end of the surgery and two times a day for four days. Only one eye of each animal (left eye) was used for the experiment. Half of the implants (9 eyes) were recellularized sheets and the other half were decellularized sheets without subsequent h-ADASC colonization. As negative controls, the contralateral eyes (right eyes) were treated using the same procedure, but without the insertion of a stromal sheet.

2.4.2. Clinical observation

Each treated eye was examined on a masked basis at 2, 4, 8 and 12 weeks after surgery, for ocular surface inflammation, transparency (T), neovascularization (N), or any complication by an experienced ophthalmologist. Neovascularization was graduated on a scale of 0–3 according to severity (0: absence; 1: peripheral and mild; 2: peripheral and moderate; 3: severe and affecting the central cornea), and the corneal transparency on a scale of 0–4 (0: total transparency and invisible implant; 1: total transparency but visible implant; 2: mild haze; 3: moderate haze; 4: severe haze making it difficult to observe the eye's internal structures).

2.4.3. Tissue procurement and histological examination

The rabbits were euthanized at 12 weeks after surgery by i.v. administration of T-61 euthanasia solution (a combination of embutramide, mebezonium iodide and tetracaine hydrochloride). The eyes were enucleated, formalin-fixed and paraffin-embedded.

Several sections of each cornea were stained with hematoxylin and eosin for light microscopy examination. The localization of CM-DiI-labeled human ADASC cells was achieved using an epifluorescence microscope.

2.4.4. Keratocan immunohistochemistry

To demonstrate differentiation into functional keratocytes, the stromal cornea-specific proteoglycan human keratocan was detected by immunohistochemistry on paraffin sections. Goat anti-human keratocan (Santa Cruz Biotechnology Inc., Santa Cruz, CA, USA) was used. Contralateral (without implant) eye sections were used as negative controls. Sections of a human cornea served as positive controls.

3. Results

3.1. Characterization of human decellularized corneal sheets

The decellularized sheets showed an opaque appearance just after the procedure (Fig. 1A) due to the detergents used, but their transparency was completely recovered after the hydration of the sheet. The weight of the native sheets was 8 ± 1.57 mg, and after decellularization treatment the weight of the sheets was 6.9 ± 0.9 mg. This difference was statistically significant ($p < 0.05$), and may be due to the extraction not only of cells, but also of extracellular matrix components such as glycosaminoglycans and water (Table 1).

The PicoGreen assay showed that the content of DNA in the native corneal sheets was 417 ± 231.2 ng/sheet, and after processing, the DNA content of corneal sheets was 9.3 ± 7.0 ng/sheet. This difference was statistically significant ($p < 0.01$) (Table 1).

The decellularization percentage obtained was 92.8% (±13.8) per sheet and 92.2% (±13.6) per milligram of tissue (Fig. 1B).

The DAPI staining did not show any cellular nuclei in the human corneal stromal sheets after the decellularization process. In contrast, many keratocyte nuclei were observed in the native corneal stromal sheets (compare Fig. 1C and D). The histology of the stained sections showed an absence of cells and a preservation of the normal fibrillar stromal architecture (not shown).

The decellularized human corneal sheets were not cytotoxic, as

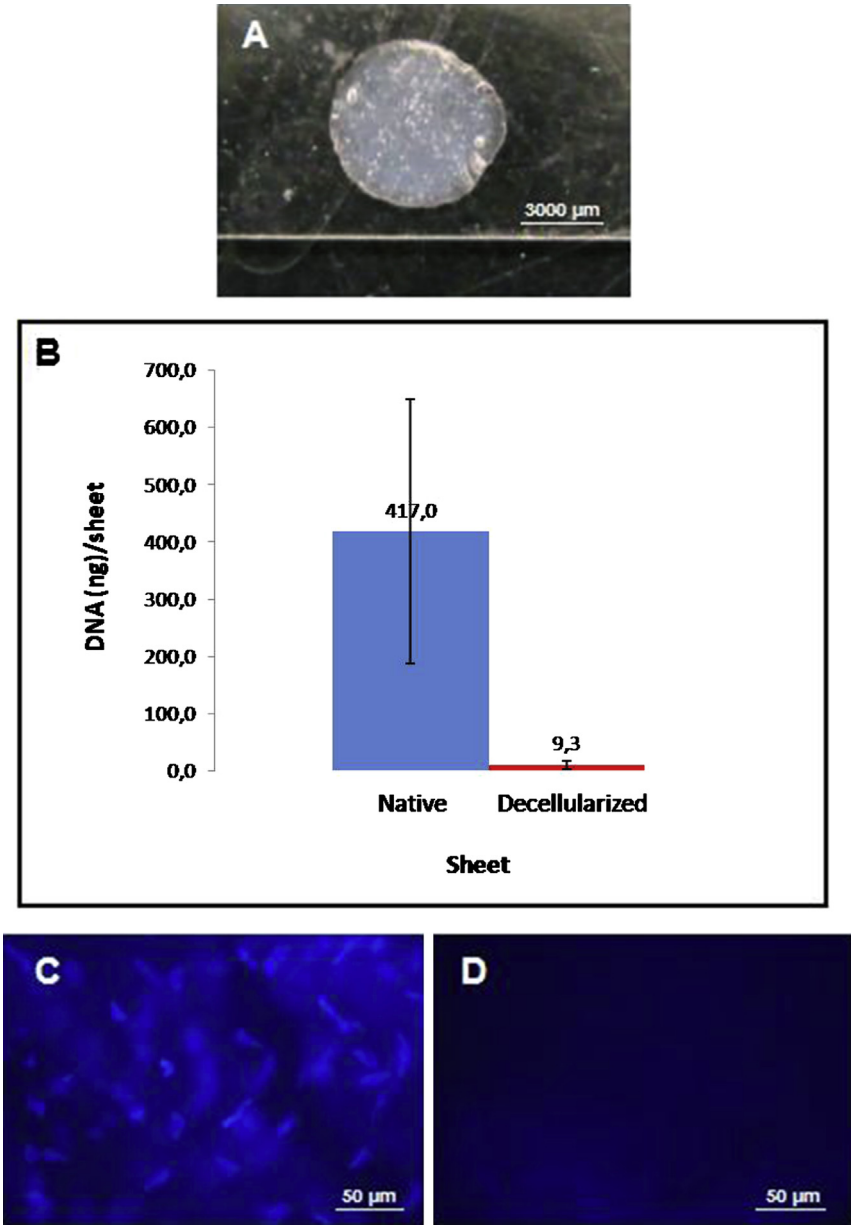

Fig. 1. A: Gross appearance of decellularized corneal sheets before their hydration. B: DNA content (ng/sheet) in native sheet matrix (blue bar) and decellularized sheet matrix (red bar). C: Fluorescence image of a native human corneal sheet stained with DAPI. D: Fluorescence image of a decellularized human corneal sheet stained with DAP. Magnification 400×. (For interpretation of the references to color in this figure legend, the reader is referred to the web version of this article.)

there was no significant difference in cell viability between the corneal sheet extract, control medium and the non-cytotoxic medium (Table 2).

3.2. Recellularization of human corneal decellularized stromal sheets

By the detection of the Vybrant CM-DiI we observed that the h-ADASC effectively colonized the surface and the inner layers of the corneal sheets after the first 24 h of culture (Fig. 2A, B). The cells did not proliferate once they colonized the sheet (no mitotic figures seen at any moment of the culture), so there were no differences on the samples cultured for 24 h respect to 5 weeks. A good

Table 1
Weight and DNA content for native and decellularized cornea.

Samples	Wet weight (mg)[a]	DNA (ng)/sheet[a]	DNA (ng)/mg tissue[a]
Native	8 ± 1.57	417.0 ± 231.2	48.1 ± 25.2
Decellularized	6.9 ± 0.9*	9.3 ± 7.0**	1.4 ± 1.1**

[a] Average ± SD; * vs native $p \leq 0.05$; ** vs native $p \leq 0.01$.

Table 2
Cytotoxicity assays. Cell viability with controls and sheet extracts.* vs control medium $p \leq 0.05$; ** control medium $p > 0.05$.

Sample	Average (% ± SD)
Control medium	100 ± 7.0
Non-cytotoxic medium	101 ± 5.3**
Cytotoxic medium 100%	7.4 ± 0.2*
Cytotoxic medium 25%	10.9 ± 0.6*
Corneal sheet extract 25%	99.4 ± 1.6**

colonization maintained during the 5 weeks of follow-up culture, showing similar high cell density while maintaining its original cellular morphology without signs of atypia (not shown). The colonization was more efficient in the sheets from the inner stroma (Fig. 2C, D), probably due to the looser compaction of collagen fibers at such depth.

3.3. Implantation of recellularized human corneal sheets in rabbit corneas

3.3.1. Surgery and clinical observation

Eighteen rabbits were used for the study, in which one eye was implanted with the sheet and the contralateral was used as a control eye. Eighteen experimental eyes (pocket with sheet) were implanted: 9 with h-ADASC (rabbits 4–12) and 9 without h-ADASC (rabbits 1–3 and 13–18). As controls, twelve control mock eyes (pocket without sheet) and six control untouched eyes were performed. All animals tolerated the procedure well, despite some complications: one case of posterior perforation toward the anterior chamber (right eye of rabbit 18) and five cases of laceration of the anterior wall of the pocket (right eye of rabbits 4, 7, 9, and left eye of rabbits 1 and 2).

The implant was completely transparent, flexible and pliable, which generated a corneal central opacity grade 0 from the time of implantation. The implant remained fully transparent during the 3-month follow-up, being nearly imperceptible clinically, except for a very subtle anterior elevation at the edges of the implant (Fig. 3A–D). The corneal peripheral transparency remained intact in all cases. In most cases, an early and mild superior peripheral neovascularization was observed (<1 mm), which was also observed in the control eyes, confined to the surgical incision site and clearly related to the suture. After the suture removal, these vessels experienced a progressive regression until their complete disappearance (N0) in the third month. In a minority of cases (rabbits 9, 11 and 12), this neovascularization was slightly larger (2–3 mm; N1). There was no sign of rejection during the follow-up in any of the eyes. None of the control eyes showed a clinical abnormality during the follow-up except the already discussed mild transient superior peripheral vessels (Fig. 3E,F).

Five cases (rabbits 3, 6, 7, 13 and 18), associated with sheets that had been stored for several weeks after decellularization and prior to culture and implantation, experienced an episode of stromal keratitis in the experimental eye within the first month after surgery. They experienced spontaneous resolution without any treatment, but leaving a moderate central opacity (T3) and a central neovascularization (N3) at the moment of euthanasia. The anterior chamber was unaffected in any case, and no case of epithelial defect, ulcer or extrusion of the implant was detected in the 3-month follow-up. Table 3 summarizes the clinical results of the 18 experimental eyes at the time of euthanasia. Differences between groups were not statistically significant for both transparency ($p = 0.340$) and vascularization ($p = 0.800$) by the nonparametric Mann–Whitney test.

3.3.2. Histological analysis of transplanted corneas

The presence of the implant was detected in the middle portion of the stroma, showing a dense band of collagen with defined edges and uniform thickness accompanied by no sign of inflammation (Fig. 4A–D) or isolated lymphocytes confined to the edges of the sheet. No deposition of crystals or neovascularization around the implant were detected. While this band was found acellular in rabbits carrying sheets without h-ADASC, as expected, in those carrying sheets with h-ADASC, a hypocellular band was observed, containing cells with stellate morphology around and inside the sheet (Fig. 4C, D). The density of cells colonizing the graft was higher in the in vitro study than in the in vivo study because of cell loss on the surface of the sheets during graft manipulation at the moment of the surgical implantation. Histologically, control eyes showed no abnormality, presenting a perfect preservation of the normal corneal anatomy (Fig. 4E, F).

In addition to the keratitis cases, two eyes (8 and 9) presented a low lymphohistiocytic inflammatory reaction around the implant

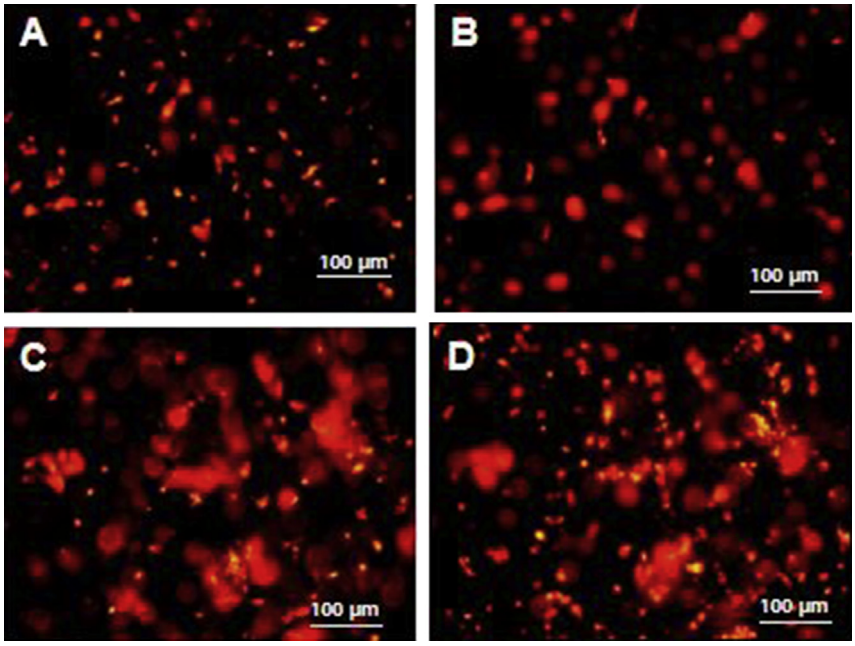

Fig. 2. A, B: Fluorescence of Vybrant CM-DiI in the same sheet at different depths 24 h after the cellular seeding. C, D: Fluorescence of Vybrant CM-DiI in the same sheet at different depths 24 h after the cellular seeding in a sheet obtained from the inner stroma (magnification 200×). Photos taken approximately at 10 µm (A, C) and 30 µm (B, D) depth from the surface of the sheet.

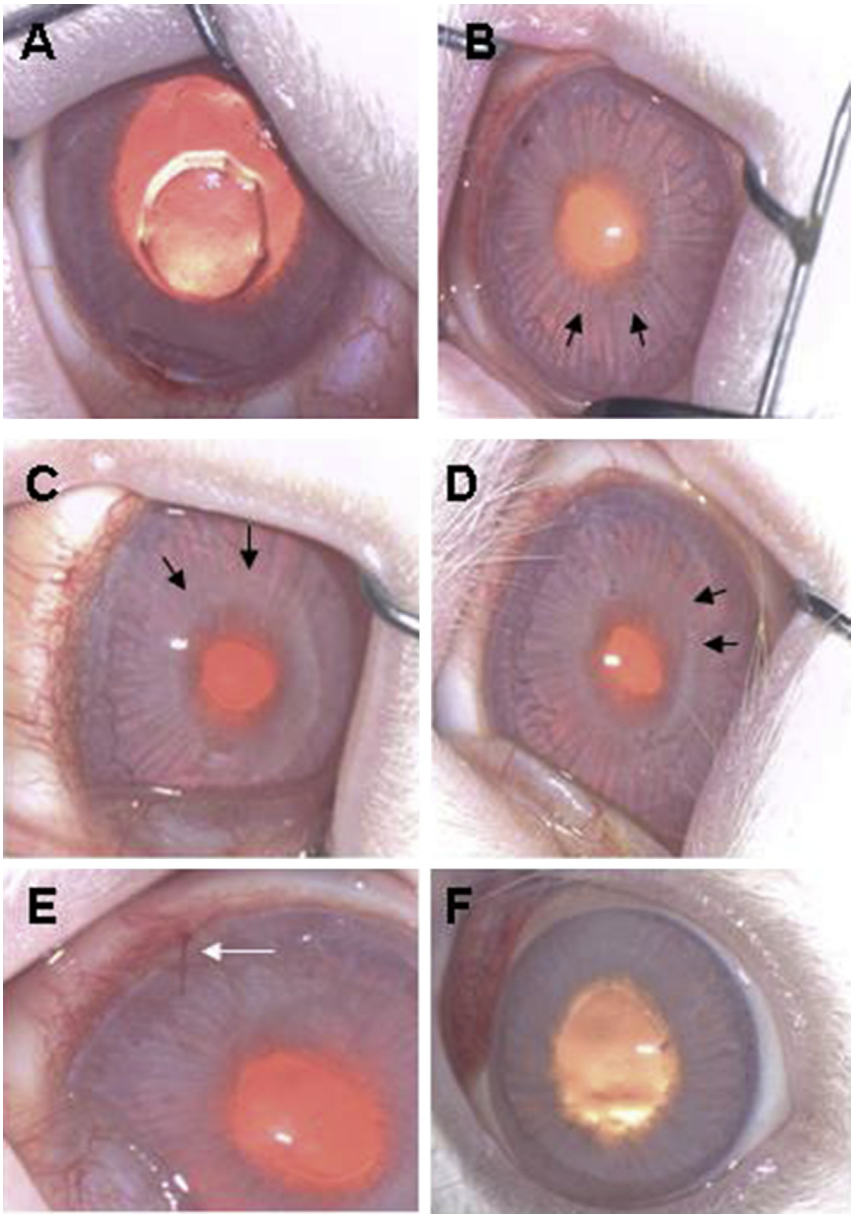

Fig. 3. Example of the transparency evolution of the sheet (rabbit 8) before (A) and after implantation and at 1 week (B), 1 month (C) and 3 months (D). The implant is transparent. Arrows point to the slightly visible edge of the sheet after implantation. None of the control eyes showed a clinical abnormality during the follow-up except a mild superior peripheral neovascularization (white arrow) at 1 week (E) that regressed at 3 months (F). Magnification: 2× except for F: 4×.

with isolated foreign body giant cells with slight edema and neovascularization. The histological patterns are summarized in Table 4. The differences between groups were not statistically significant ($p = 0.547$) by the nonparametric Mann–Whitney test. Control eyes showed no histological abnormality, presenting a perfect preservation of the normal corneal anatomy (Fig. 4E, F).

3.3.3. Fluorescence of Vybrant CM-DiI and keratocan production by transplanted h-ADASC

To determine that the cellularity in the recellularized human stromal sheets was actually composed of h-ADASC and not of rabbit cells infiltrating the implant, we assayed the detection of the Vybrant CM-DiI by epifluorescence microscopy. We observed that the nine corneas with recellularized implants presented strongly positive cells distributed around and inside the sheet (Fig. 5E). Vybrant CM-DiI was not detected in either of the negative controls or in the experimental eyes with uncellularized sheets.

Moreover, human keratocan was found to be expressed by the transplanted human cells in all nine cases, confirming the keratocytic differentiation of some of the h-ADASC (Fig. 5F). Human keratocan protein was not detected in either of the negative controls or in the experimental eyes with uncellularized sheets (Fig. 5B).

4. Discussion

In the last few years, corneal decellularized matrices have gained attention because they provide a more natural environment for the growth and differentiation of cells when compared with synthetic scaffolds. We observed that the DNA content in native sheets shows high variability owing to the fact that keratocyte density in a normal human cornea is the highest in the zone adjacent to Bowman's layer and decreases slightly through the

Table 3
Clinical results of experimental eyes at the end of follow-up.

n:18	Extrusion	Cases without extrusion								
		Transparency					Vascularization			
		0	1	2	3	4	0	1	2	3
Sheets + h-ADASC (n:9)	0	7			2		5	2		2
Sheets − h-ADASC (n:9)	0	5	1		2	1	6		1	2

remaining depth of the stroma. The variability in keratocyte population between individuals should also be taken into account (Patel et al., 2001). The effectiveness of SDS decellularization in the human cornea has previously been demonstrated, although in several publications it has been reported that detergents can induce damage to the human corneal epithelial basement membrane, consequently affecting epithelial growth but not fibroblast growth (Crapo et al., 2011; Shafiq et al., 2012; Choi et al., 2010). In our study, we have considered tissue under the following conditions as a valid acellular ECM: 1) Quantity of DNA less than 50 ng/mg of tissue; 2) Conserved extracellular matrix architecture; 3) Recolonizable in both in vitro and in vivo assays.

The keratocytes in the corneal stromal cellular compartment are essential for remodeling the stroma because they produce the proteoglycans and metalloproteinases essential for the long-term maintenance of corneal transparency (Lynch and Ahearne, 2013). In addition, stromal–epithelial interactions are key determinants of corneal function (Liu et al., 1999). This highlights the importance of transplanting a cellular substitute together with the structural support. To the best of our knowledge, all attempts to repopulate decellularized corneal scaffolds have used corneal cells (Shafiq et al., 2012), but these cells have major drawbacks that preclude their autologous use (damage of the donor tissue, lack of cells and inefficient cell subculture), thus forcing efforts to find an extra-ocular source of autologous cells. In our study, we have used h-ADASC to repopulate our scaffolds, which have been demonstrated

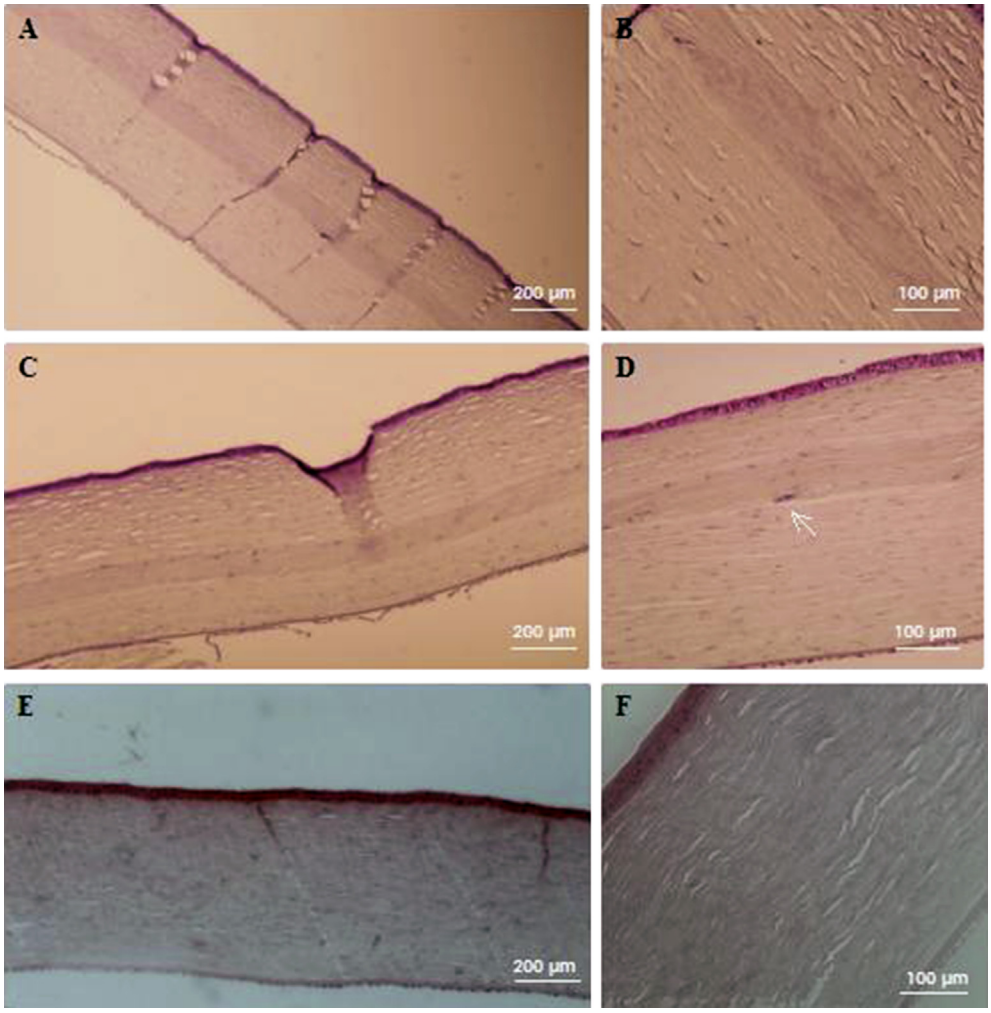

Fig. 4. Hematoxylin-eosin staining of rabbits corneas: rabbit 1 (no h-ADASC) (A, B): acellular band without vessels or any inflammatory sign; rabbit 10 (C) and 11 (D) (with h-ADASC): hypocellular band without vessels or any inflammatory sign (B). In some cases (D) some presumable inflammatory cells were observed (arrow). Control eyes showed no histological abnormality (E, F). Magnification 100× (A, C, E); Magnification 200× (B, D, F).

Table 4
Inflammatory infiltrate tissue depending on the presence or absence of h-ADASC.

n:18	Inflammatory infiltrate tissue				
	None	Minimal	Mild	Moderate	Severe
Sheet + h-ADASC (n:9)	3	2	0	2	2
Sheet − h-ADASC (n:9)	4	3	0	0	2

to be a perfect source of autologous stem cells for the development of tissue-engineered corneas, avoiding the limitations of corneal cells (De Miguel et al., 2010; Arnalich-Montiel et al., 2008; Martínez-Conesa et al., 2012).

Due to shortage of corneas for experimental purposes, only DNA content, cytotoxicity and cell survival were tested in decellularized corneas ex vivo. However, due to the nature of the decellularization buffers used, we can anticipate that collagen concentration does not vary at all with this decellularization protocol, whereas all proteoglycans will be dissolved away. Overall structure does not change due to the preserved collagen content and already

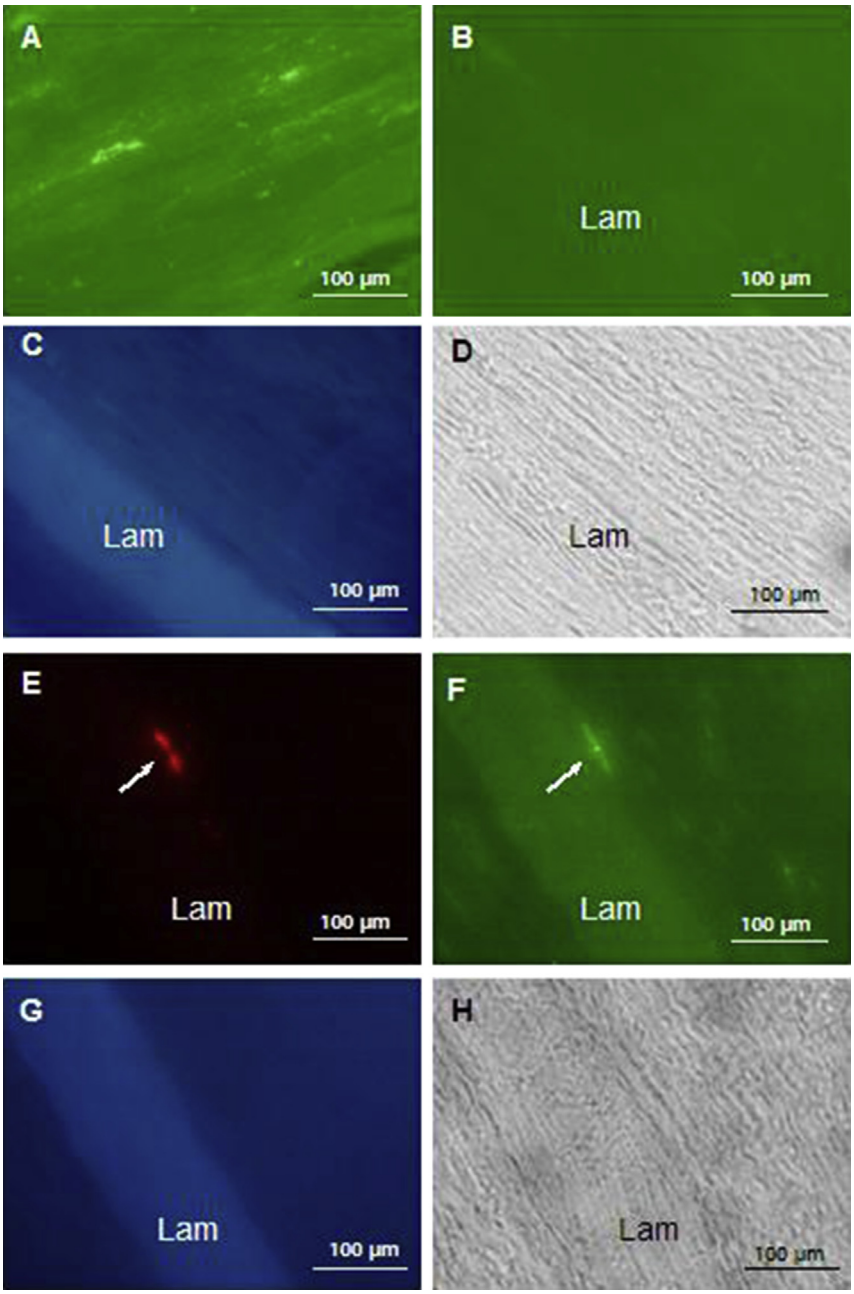

Fig. 5. Human keratocan immunofluorescence. A: Positive control of human keratocan immunofluorescence in a human cornea showing keratocytes in green. B: Human keratocan immunofluorescence in a rabbit cornea with decellularized lamina (lam), showing no immunoreaction to human keratocan. C: Same zone as in B showing DAPI staining in blue demonstrating no cell migration inside the lamina. D: Same zone as in B showing phase contrast image where histological integration of the lamina is demonstrated. E: Fluorescent CM-Dil-labeled human cells (red, arrow) in the re-cellularized lamina with h-ADSC. F: Same zone as in E showing human cells in the lamina (lam) and their differentiation into human keratocytes (arrow, green keratocan labeling). G: Same zone as in E showing DAPI staining in blue demonstrating no host cell migration inside the lamina. H. Same zone as in E showing phase contrast image where histological integration of the lamina is demonstrated. Magnification 400×. (For interpretation of the references to color in this figure legend, the reader is referred to the web version of this article.)

established alignment in parallel of the collagen fibers. This could account for the lack of differentiation of h-ADASC into keratocytes during cell culture, as demonstrated previously by our group (Arnalich-Montiel et al., 2008), so this fact could be only observed in the in vivo samples.

The clinical results obtained were excellent, with maintenance of a full transparency without any sign of scarring throughout the follow-up. In most cases, the implant was only visible by a minimal elevation of the anterior corneal surface at the edges of the sheet. In several cases, we detected a slight peripheral and superior vascularization, also seen in the controls, directly related to the corneal incision. We believe this is connected not with the implant itself, but with the proximity of the surgical incision to the limbal vessels, as in normal rabbits the superior limbus appears widely vascularized because of a very anterior insertion of the superior rectus muscle. Therefore, this should be avoided with a superotemporal incision in subsequent experiments.

We did not see host cells migrating toward the implant, which remained acellular (in non h-ADASC group) during the 3-month follow-up, in contrast to other studies (Lynch and Ahearne, 2013; Xu et al., 2008). This lack of host cell migration has also been reported in some publications using decellularized porcine corneas (Amano et al., 2008; Hashimoto et al., 2010). This can be explained by the lack of chemoattracting signals from the decellularized implant; however, we cannot discard a host cell migration with a longer follow-up.

Also, despite using immune-competent animals and a xenogeneic graft, the h-ADASC did not elicit an immune response in the surrounding tissue, as also demonstrated in a previous publication of our group (Arnalich-Montiel et al., 2008). This fact can be explained by the immunoprivilege properties of these cells. However, they were incompetent enough to immunomodulate the two cases of stromal keratitis that occurred in the h-ADASC group, showing the same clinical outcome as the three cases in the non-h-ADASC group.

The cases of stromal keratitis were all associated with sheets that had been stored for several weeks after decellularization and prior to implantation, which presented with an abnormal increased rigidity. These isolated cases appeared independent of the presence or absence of stem cells, and the rest of the experimental cases showed an excellent clinical response to the implant, so we believe these cases are not directly related to the decellularized stroma or the stem cells. A shortening of the period between the decellularization of the donor cornea and its implantation should help to avoid this undesired complication. The changes of mechanical properties over time would be very interesting for subsequent studies in order establish a time frame for transplantation in humans. We did not appreciate increase in rigidity in the in vitro study after 5 weeks, but the storage period was longer than three months for the sheets used for the in vivo study whose rigidity increase was appreciated, so at this time we can advice a time frame for transplantation lower than 5 weeks.

Despite slightly better clinical results in the h-ADASC group, there were no statistically significant differences between both groups. This is probably due to the great integration already achieved by the decellularized human sheet in the rabbit corneal stroma. Moreover, some of the transplanted h-ADASC did in fact differentiate into human keratocytes, as demonstrated by the expression of human keratocan, but not all of them, so the lack of differences between the groups could also be due to this low efficiency of differentiation of h-ADSC into keratocytes by simply injecting them into decellularized corneas. It will be interesting to increase such differentiation efficiency by isolating subgroups of ADSC with higher differentiation potential or by pre-differentiating them in vitro previous to the transplant.

We have demonstrated that transplanted h-ADASC inside a human decellularized stromal graft survive at least 12 weeks after the transplant, remaining intermingled between the donor stromal collagen layers without disrupting its histological pattern; they also differentiate into human keratocytes, as previously demonstrated when h-ADASC were injected alone into rabbit stroma or in a hyaluronic scaffold (Arnalich-Montiel et al., 2008; Espandar et al., 2012). Therefore, with this model of lamellar transplant, we would be able to obtain an autologous graft for patients using only a sample of their adipose tissue and an allogeneic donor cornea, avoiding the risk of stromal rejection associated with current surgical options of lamellar transplant, although this will require further research to be demonstrated. As the graft is inserted inside a stromal pocket, the epithelial and endothelial layers are not modified, avoiding their rejection and shortening the postsurgical recovery. The possible clinical applications of this model of lamellar transplant would be mainly focused on ectasias and other corneal debilitating diseases, replacing DALK in patients with severe stromal thinning but without significant corneal scarring. It would also be possible to obtain several grafts from a unique allogeneic donor cornea, increasing the availability of donor tissue and shortening waiting lists.

In conclusion, we report a new model of lamellar transplant that requires only a simple and safe procedure of liposuction and a donor untransplantable cornea to provide an optically transparent autologous stromal graft with demonstrated excellent biocompatibility and integration into the host tissue in a rabbit model, which might avoid complications associated with current techniques, and therefore would improve the patients' visual prognosis and quality of life.

Conflicts of interest

The authors, their families, their employers and their business associates have no financial or proprietary interest in any product or company associated with any device, instrument or drug mentioned in this article. The authors have not received any payment as consultants, reviewers or evaluators of any of the devices, instruments or drugs mentioned in this article.

Acknowledgments

This work was supported in part by grants CEN-20091021 from the Spanish Ministry of Health, IAP-560610-2008-44 and SAF2010-19230 from the Spanish Ministry of Science and Innovation, and from Fundació Marató de TV3, Spain. We thank Fátima Domínguez (CEL) and Vissum opthalmologists Felipe Soria Arrellano, Alessandro Abouda and Amr el Aswad for technical help, and Juliette Siegfried (ServingMed.com) for the English editing of this manuscript.

References

Amano, S., Shimomura, N., Yokoo, S., et al., 2008. Decellularizing corneal stroma using N_2 gas. Mol. Vis. 14, 878–882.
Arnalich-Montiel, F., Pastor, S., Blazquez-Martinez, A., et al., 2008. Adipose-derived stem cells are a source for cell therapy of the corneal stroma. Stem Cells 26 (2), 570–579.
Carlson, E.C., Liu, C.Y., Chikama, T., et al., 2005. Keratocan, a cornea-specific keratan sulfate proteoglycan, is regulated by lumican. J. Biol. Chem. 280, 25541–25547.
Choi, J.S., Williams, J.K., Greven, M., et al., 2010. Bioengineering endothelialized neocorneas using donor-derived corneal endothelial cells and decellularized corneal stroma. Biomaterials 31 (26), 6738–6745.
Crapo, P.M., Gilbert, T.W., Badylak, S.F., 2011. An overview of tissue and whole organ decellularization processes. Biomaterials 32 (12), 3233–3243.
Daniel, J., Abe, K., McFetridge, P.S., 2005. Development of the human umbilical vein scaffold for cardiovascular tissue engineering. ASAIO J. 51, 252–261.
De Miguel, M.P., Alió, J.L., Arnalich-Montiel, F., Fuentes-Julian, S., de Benito-Llopis, L.,

Amparo, F., Bataille, L., 2010. Cornea and ocular surface treatment. In: Current Stem Cell Research and Therapy. Special Issue: Adipose-derived Stem Cells, 5, pp. 195–204 (Chapter 17).
De Miguel, M.P., Fuentes-Julián, S., Blázquez-Martínez, A., et al., 2012. Immunosuppressive properties of mesenchymal stem cells: advances and applications. Curr. Mol. Med. 12 (5), 574–591.
Espandar, L., Bunnell, B., Wang, G.Y., et al., 2012. Adipose-derived stem cells on hyaluronic acid-derived scaffold: a new horizon in bioengineered cornea. Arch. Ophthalmol. 130 (2), 202–208.
Fang, B., Song, Y., Liao, L., et al., 2007. Favorable response to human adipose tissue-derived mesenchymal stem cells in steroid-refractory acute graft-versus-host disease. Transpl. Proc. 39 (10), 3358–3362.
Griffith, M., Hakim, M., Shimmura, S., et al., 2002. Artificial human corneas: scaffolds for transplantation and host regeneration. Cornea 21 (7 Suppl. l), S54–S61.
Hashimoto, Y., Funamoto, S., Sasaki, S., et al., 2010. Preparation and characterization of decellularized cornea using high-hydrostatic pressurization for corneal tissue engineering. Biomaterials 31 (14), 3941–3948.
Krumeich, J.H., Knulle, A., Krumeich, B.M., 2008. Deep anterior lamellar (DALK) vs penetrating keratoplasty (PKP) a clinical and statistical analysis. Klin. Monbl Augenheilkd. 225 (7), 637–648.
Liu, J., Wilson, S., Mohan, R., 1999. Stromal-epithelial interactions in the cornea. Prog. Retin Eye Res. 18 (3), 293–309.
Lynch, A.P., Ahearne, M., 2013. Strategies for developing decellularized corneal scaffolds. Exp. Eye Res. 108, 42–47.
Martínez-Conesa, E.M., Espel, E., Reina, M., Casaroli-Marano, R.P., 2012. Characterization of ocular surface epithelial and progenitor cell markers in human adipose stromal cells derived from lipoaspirates. Invest Ophthalmol. Vis. Sci. 53 (1), 513–520.
McFetridge, P.S., Daniel, J.W., Bodamyali, T., Horrocks, M., Chaudhuri, J.B., 2004. Preparation of porcine carotid arteries for vascular tissue engineering applications. J. Biomed. Mater. Res. 70A, 224–234.
Michelacci, Y.M., 2003. Collagens and proteoglycans of the corneal extracellular matrix. Braz J. Med. Biol. Res. 36, 1037–1046.
Patel, S., McLaren, J., Hodge, D., Bourne, W., 2001. Normal human keratocyte density and corneal thickness measurement by using confocal microscopy in vivo. Invest Ophthalmol. Vis. Sci. 42 (2), 333–339.
Ponce Márquez, S., Martínez, V.S., et al., 2009. Decellularization of bovine corneas for tissue engineering applications. Acta Biomater. 5 (6), 1839–1847.
Puissant, B., Barreau, C., Bourin, P., et al., 2005. Immunomodulatory effect of human adipose tissue-derived adult stem cells: comparison with bone marrow mesenchymal stem cells. Br. J. Haematol. 129 (1), 118–129.
Ruberti, J.W., Zieske, J.D., 2008. Prelude to corneal tissue engineering - gaining control of collagen organization. Prog. Retin Eye Res. 27 (5), 549–577.
Shafiq, M.A., Gemeinhart, R.A., et al., 2012. Decellularized human cornea for reconstructing the corneal epithelium and anterior stroma. Tissue Eng. Part C Methods 18 (5), 340–348.
Shao, Y., Quyang, L., Zhou, Y., et al., 2010. Preparation and physical properties of a novel biocompatible porcine corneal acellularized matrix. In Vitro Cell Dev. Biol. Anim. 46 (7), 600–605.
Shao, Y., Yu, Y., Pei, C.G., et al., 2012. Evaluation of novel decellularizing corneal stroma for cornea tissue engineering applications. Int. J. Ophthalmol. 5 (4), 415–418.
Shimmura, S., Tsubota, K., 2006. Deep anterior lamellar keratoplasty. Curr. Opin. Ophthalmol. 17, 349–355.
Watson, S.L., Tuft, S.J., Dart, J.K., 2006. Patterns of rejection after deep lamellar keratoplasty. Ophthalmology 113 (4), 556–560.
Xu, Y.G., Xu, Y.S., Huang, C., et al., 2008. Development of a rabbit corneal equivalent using an acellular corneal matrix of a porcine substrate. Mol. Vis. 14, 2180–2189.
Zuk, P.A., Zhu, M., Mizuno, H., et al., 2001. Multilineage cells from human adipose tissue: implications for cell-based therapies. Tissue Eng. 7, 211–228.